


MPA-MutPred: a novel strategy for accurately predicting the binding affinity change upon mutation in membrane protein complexes

Fathima Ridha and M. Michael Gromiha *

Department of Biotechnology, Bhupat and Jyoti Mehta School of Biosciences, Indian Institute of Technology Madras, Chennai 600036, India

*Corresponding author. Department of Biotechnology, Bhupat and Jyoti Mehta School of Biosciences, Indian Institute of Technology Madras, Chennai 600036, India.

E-mail: gromiha@iitm.ac.in

Abstract

Mutations in the interface of membrane protein (MP) complexes are key contributors to a broad spectrum of human diseases, primarily due to changes in their binding affinities. While various methods exist for predicting the mutation-induced changes in binding affinity ($\Delta\Delta G$) in protein–protein complexes, none are specific to MP complexes. This study proposes a novel strategy for $\Delta\Delta G$ prediction in MP complexes, which combines linear and nonlinear models, to obtain a more robust model with improved prediction accuracy. We used multiple linear regression to extract informative features that influence the binding affinity in MP complexes, which included changes in the stability of the complex, conservation score, electrostatic interaction, relatively accessible surface area, and interface contacts. Further, using gradient boosting regressor on the selected features, we developed MPA-MutPred, a novel method specific for predicting the $\Delta\Delta G$ of membrane protein–protein complexes, and it is freely accessible at <https://web.iitm.ac.in/bioinfo2/MPA-MutPred/>. Our method achieved a correlation of 0.75 and a mean absolute error (MAE) of 0.73 kcal/mol in the jack-knife test conducted on a dataset of 770 mutants. We further validated the method using a blind test set of 86 mutations, obtaining a correlation of 0.85 and an MAE of 0.77 kcal/mol. We anticipate that this method can be used for large-scale studies to understand the influence of binding affinity change on disease-causing mutations in MP complexes, thereby aiding in the understanding of disease mechanisms and the identification of potential therapeutic targets.

Keywords: membrane proteins; mutation; binding affinity change; structure-based features; sequence-based features

Introduction

Membrane proteins (MPs) are an essential group of proteins making up ~20%–30% of the human proteome [1]. Their significance lies in their diverse functions as molecular transporters, signal receptors, ion channels, and enzymes, rendering them primary targets for medicinal drugs [2]. Membrane proteins mostly function as complexes, and the strength of their binding (binding affinity), quantified by binding free energy (ΔG), is critical for their proper functioning. However, due to their complex structural characteristics, the binding affinity of MPs has been less extensively studied compared to globular proteins. Recently, Ridha *et al.* [3] developed a machine learning (ML)-based method, MPA-Pred, to predict the binding affinity of MP–protein complexes using structure- and sequence-based features. It was observed that aromatic and charged residues at the interface and noncovalent interactions such as electrostatic interactions play a crucial role in understanding the MP binding affinity [4].

On the other hand, changes in binding affinity resulting from mutations can disrupt vital processes, leading to aberrant cellular function and potential disease onset [3]. Mutations in MPs have been implicated as the culprits across a broad range of human

diseases, including cancers, cardiovascular conditions, congenital disorders, and more [5]. For instance, mutations in voltage-gated ion channels (VGICs) can lead to cardiac dysfunction, as seen with the KCNH2 mutation (N588K) causing sudden cardiac death [6]. Similarly, mutations in membrane-bound receptors, like the L858R mutation in the epidermal growth factor receptor, drive carcinogenesis, particularly in lung cancer [7]. Hence, it is important to understand the mutational effects on the binding affinity in MPs.

Quantitatively, the influence of mutations is determined by the change in binding free energy ($\Delta\Delta G$), using various experimental techniques. Recently, Ridha *et al.* [8] compiled data on experimental binding affinity change upon mutation from literature and developed a database, Membrane Protein complex binding Affinity Database (MPAD), which includes ~5400 affinity data. However, due to the resource-intensive and time-consuming nature of experimental techniques, they are not feasible for large-scale studies. Consequently, computational methods become indispensable for predicting changes in the binding affinity of MP complexes resulting from mutations.

Recent years have seen the emergence of various computational approaches, predominantly employing machine learning

Received: July 4, 2024. Revised: October 10, 2024. Accepted: November 4, 2024

© The Author(s) 2024. Published by Oxford University Press.

This is an Open Access article distributed under the terms of the Creative Commons Attribution Non-Commercial License

(<https://creativecommons.org/licenses/by-nc/4.0/>), which permits non-commercial re-use, distribution, and reproduction in any medium, provided the original work is properly cited. For commercial re-use, please contact journals.permissions@oup.com

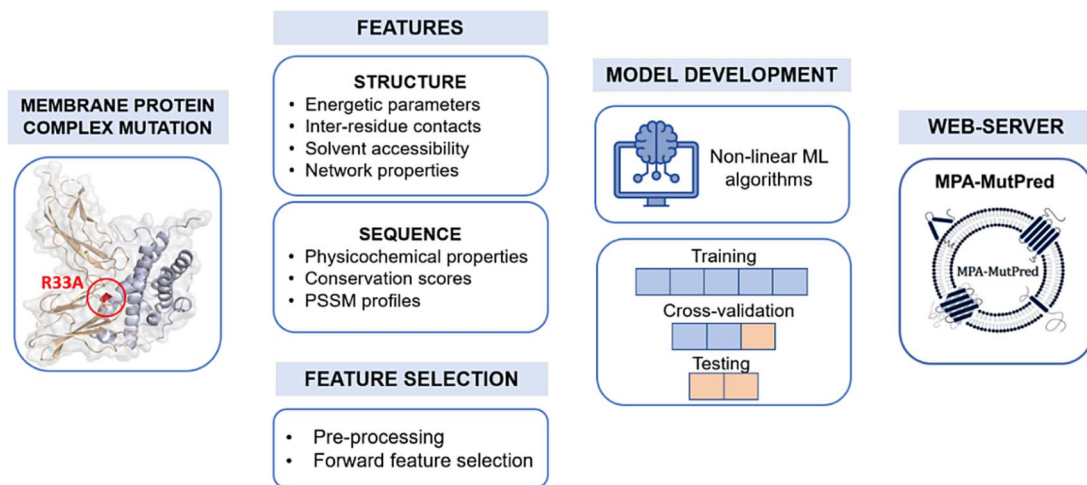


Figure 1. An overview showing the workflow of MPA-MutPred methodology.

and deep learning, to efficiently predict changes in binding affinity upon mutation, leveraging both structural and sequence-based features [9–16]. However, these methods are designed for protein–protein complexes in general and do not account for the unique challenges posed by MPs. We also observed that most mutations occurred in the extracellular and/or cytoplasmic regions of the MP–protein complex. On the other hand, such mutations can significantly influence MP–protein interactions by potentially altering the conformation of the membrane-spanning regions, thus disrupting the key function [3, 17]. Although it is similar to mutations in globular proteins, existing prediction methods for globular proteins exhibit poor performance in predicting $\Delta\Delta G$ values for MPs due to distinct structural and environmental characteristics. This highlights the need for a specific method to predict affinity change upon mutation in MP–protein complexes, which is currently lacking in the literature.

To bridge this gap, we introduce a new method for predicting the changes in binding free energy of MP–protein complexes caused by single mutations (Fig. 1). Our distinctive approach integrates complementary ML algorithms, offering a synergistic solution to enhance the prediction of changes in binding affinity upon mutation, leading to a more robust predictive model. We developed a prediction model using multiple linear regression (MLR) for feature selection, followed by gradient boosting regressor (GBR), achieving a correlation of 0.75 and a mean absolute error (MAE) of 0.73 kcal/mol in the jack-knife test and a correlation of 0.85 with an MAE of 0.77 kcal/mol on the blind test set. We also identified the important features influencing the binding affinity change in MP complexes and performed SHAP (SHapley Additive exPlanations) analysis to elucidate their contribution to the model predictions, enhancing the interpretability of our approach. A user-friendly web server, MPA-MutPred, was also developed, which is freely accessible for public use. The selected features and model development approach will be discussed in detail.

Materials and methods

Dataset

The MPAD database [8] is utilized to obtain reliable single mutation data on the binding affinity of MP complexes with known wild-type and mutant ΔG values. We then calculated the binding

free energy change using Equation (1),

$$\Delta\Delta G = \Delta G_{\text{mut}} - \Delta G_{\text{wt}} \quad (1)$$

where ΔG_{wt} and ΔG_{mut} represent the binding free energies of the wild-type and mutant complex, respectively. In our study, an increase in binding affinity is indicated by a negative $\Delta\Delta G$ value, while a positive $\Delta\Delta G$ value signifies a decrease in affinity, independent of the magnitude.

Additionally, to balance the skewed distribution of $\Delta\Delta G$ in the dataset, we included hypothetical reverse mutations [18], where the $\Delta\Delta G$ of a mutation from wild type to its mutant is considered to be equal to the negative of the change in binding affinity from mutant to wild type.

$$\Delta\Delta G (\Delta G_{\text{mut}} - \Delta G_{\text{wt}}) = -\Delta\Delta G (\Delta G_{\text{wt}} - \Delta G_{\text{mut}}) \quad (2)$$

This approach, widely used in the literature [9, 10, 16] helps to achieve a more balanced representation of the dataset, thereby enhancing the model’s generalizability and predictive performance. Including the hypothetical reverse mutations, the total dataset consists of 856 mutations, of which 770 were utilized to train the final model. Further, we utilized 86 single mutations (90:10 split) as the blind test set to evaluate the performance of the model.

Feature extraction

Structure-based features

We obtained the wild-type complex structures from the Protein Data Bank (PDB) and employed the BuildModel function in FoldX [19] to introduce single-point mutations into the wild-type crystal structure from PDB, in order to generate the mutant complex. Using the wild and the mutant structures, we calculated several structure-based features, which include: (i) energetic parameters obtained using FoldX; (ii) accessible surface area using NACCESS program [20]; (iii) residue depth analysis with Bio.PDB package, (iv) hydrogen bond features from HBPLUS [21]; (v) network properties using network package [22]; (v) interface residue–based contacts with 5.5 Å cutoff; and (vi) label-encoded features related to the mutation site such as chemical properties, size, and polarity of the residues [12].

Sequence-based features

We calculated several sequence-based features, including: (i) physicochemical properties, distance potentials, and mutation matrices from AAIndex [23]; (ii) conservation scores using AACon [24]; and (iii) Position-Specific Scoring Matrix (PSSM) scores using PSI-BLAST.

Feature selection

The features computed for each mutation were subject to preprocessing to avoid overfitting and eliminate redundant features. Initially, interfeature correlations were assessed, and highly correlated features ($r > 0.7$) were systematically removed. Among the two features showing high correlation, the one less correlated with the response variable was eliminated, thus ensuring a reduced set of features with minimal multicollinearity and maximal relevance to the target variable.

Following preprocessing, the sequential forward feature selection (FFS) procedure was employed to identify the important features essential for achieving the highest predictive performance of the model. Initially, an extensive systematic search was conducted to evaluate all possible five feature combinations. The top-performing combination was then used in an FFS process, where the number of features in each combination was increased by one to incorporate additional features. The process continued until adding new features no longer improved the correlation (r) or reduced the MAE.

Model development

The complete workflow containing feature preprocessing, feature selection using MLR, and the training and evaluation of the prediction method using GBR is illustrated in [Supplementary Figure S1](#). Initially, the multivariate linear regression method was used to select the features based on the performance (see [Feature Selection](#) section).

After performing forward feature selection, the selected combination of features (see the [Results](#) section for details) was used to train the prediction model. We employed various ML algorithms to assess their performance ([Supplementary Table S1](#)). Based on the performance, we selected the “GradientBoostingRegressor” from the “ensemble” module in the Scikit-learn toolkit [25] for the implementation of the final prediction model.

Performance evaluation

To evaluate the model performance, we used the Pearson correlation coefficient (r) and assessed the prediction errors using the mean absolute error (MAE) [3]. Furthermore, the robustness of the trained model was evaluated using 10-fold cross-validation and a jack-knife test. In the jack-knife test, the model is trained using $n - 1$ data points, and the $\Delta\Delta G$ for the excluded data point is then predicted. This process is repeated for each of the n data points. We also conducted an additional validation of our model using an independent test dataset.

Results and Discussion

Statistics of the dataset

We analyzed the binding affinity change of 770 mutations, and the distribution of $\Delta\Delta G$ ranged from -6.1 to 6.1 kcal/mol ([Supplementary Figure S2](#)). We found that 57.5% of the mutations changed the binding affinity by ± 1 kcal/mol. Additionally, 20.2% of the mutations enhanced binding affinity ($\Delta\Delta G < -1$ kcal/mol), and 22.3% led to a reduction in affinity ($\Delta\Delta G > 1$ kcal/mol).

Notably, the mutation R33Q in interferon alpha-2 (IFN α 2) significantly impacted its binding affinity with interferon alpha receptor 2 (ifnar2). The wild-type complex demonstrated a binding free energy of -11.62 kcal/mol. The positive charge of the arginine side chain allows it to engage in strong electrostatic interactions with negatively charged residue (Asp 51) on ifnar2, contributing significantly to the affinity and stability of the IFN α 2-ifnar2 complex [26]. Mutation to glutamine (R33Q) resulted in a ΔG of -5.54 kcal/mol, significantly lowering the affinity ($\Delta\Delta G = 6.1$ kcal/mol) due to the loss of electrostatic interactions at the binding interface. Another example is the Y13A mutation in human interleukin-4 binding protein (IL4-BP), which significantly reduced its binding affinity for interleukin-4 (IL-4) with a $\Delta\Delta G$ of 5.2 kcal/mol. The substantial loss of affinity in this variant is likely due to structural perturbations, as the aromatic ring of Y13 is fully buried within the protein [27].

Nonlinear methods using features obtained from regression improved the $\Delta\Delta G$ prediction

We used the FFS method combined with multiple linear regression to identify the optimal features with the best predictive performance. Our iterative process initiated with all 5 feature combinations and progressively extended up to 12 features using the FFS method for the final model, as there was no significant improvement in the performance beyond 12 features. Using these selected features, we examined the performance on an MLR model and obtained a correlation of 0.74 and an MAE of 0.75 kcal/mol in training and a correlation of 0.73 with an MAE of 0.76 kcal/mol in the jack-knife test. Further, we compared the performance on six different machine learning algorithms, and the results are provided in [Supplementary Table S1](#). Inspection of the results revealed that the GBR showed improved performance compared to the other methods, with a correlation up to 0.75 and a reduction of MAE to 0.73 kcal/mol during the jack-knife test.

When we evaluated the performance of the model directly trained on the entire feature set using the GBR, we obtained a reduced performance ($r = 0.72$ and MAE = 0.76 kcal/mol in the jack-knife test) in comparison to our previous approach. Also, feature selection using the GBR is time-consuming and computationally expensive, especially with a large number of features. This suggests that incorporating feature selection through linear regression helps to reduce complexity, potentially improves interpretability, and can lead to better model performance. Thus, we employed a novel approach of using linear regression for feature selection followed by training gradient boosting on the selected features, to obtain a more robust model by leveraging the strengths of both approaches for improved performance.

Performance on training and cross-validation

We used both default parameters and hyperparameter tuning using the GridSearchCV method with a 5-fold cross validation (CV) to compare the performance. We tested different hyperparameter values: `n_estimators`: 100, 200, 300; `learning_rate`: 0.01, 0.1, 1.0, 10; `max_depth`: 1, 3, 5, 7, 9; and `sub_sample`: 0.5, 0.8, 1.0. However, the model with default parameters (`n_estimators = 100`, `learning_rate = 0.1`, `max_depth = 3`, `subsample = 1.0`) clearly outperformed the tuned model ([Supplementary Table S2](#)). Hence, we finalized the GBR model with default parameters.

The method demonstrated a training correlation of 0.91 with an MAE of 0.49 kcal/mol, while the jack-knife test results showed a correlation of 0.75 and an MAE of 0.73 kcal/mol ([Fig. 2a](#)). Further, in 10-fold cross-validation, the model predicts $\Delta\Delta G$ with a

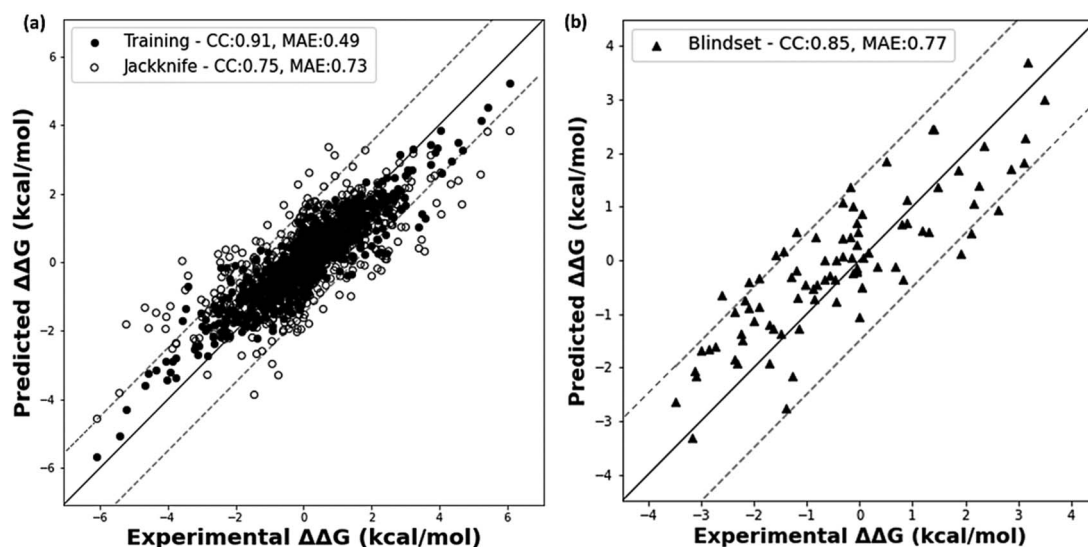


Figure 2. Regression plots depicting the relationship between experimental and predicted $\Delta\Delta G$ on (a) training and jack-knife test and (b) blind test set. The dotted line represents the mutations predicted with a deviation of ± 1.5 kcal/mol.

correlation of 0.74 and an MAE of 0.75 kcal/mol (Supplementary Figure S3).

Performance on blind test

We tested our model on a blind dataset consisting of 86 mutations to evaluate its prediction performance. The model achieved an MAE of 0.77 kcal/mol and a correlation of 0.85 between the experimental and predicted binding affinities. Figure 2b illustrates the relationship between the actual and predicted $\Delta\Delta G$ values for the test set. For instance, the mutation F269A in interferon lambda receptor 1 (IFNLR1) interacting with tyrosine-protein kinase JAK1 (PDB: 5IXD) resulted in a $\Delta\Delta G$ of 3.50 kcal/mol. The method is able to accurately predict the binding affinity change of the complex (3.98 kcal/mol) within a deviation of 0.48 kcal/mol.

Performance across different functional classes

We have developed a generic model by considering mutations in all classes of MPs together. For assessing the generalizability of the model in different functional classes, we evaluated its performance on each class separately in a jack-knife test and an external blind dataset (Supplementary Figure S4). Notably, the model performed well across all classes, achieving an MAE of <1 kcal/mol, with specific values of 0.70, 0.74, 0.87, and 0.63 kcal/mol for mutations in enzymes, receptors, transporters, and miscellaneous proteins, respectively, in the jack-knife set. This could be due to the fact that the selected features such as change in total energy and conservation score are shown to be important in all classes of proteins. Further, we noticed a minor difference in performance across different classes, and it might be due to the following reasons: (i) the model is trained on a broad $\Delta\Delta G$ range of -6 to $+6$ kcal/mol, while specific functional classes, such as transporters, have a narrow $\Delta\Delta G$ range of -2 to $+2$ kcal/mol, and (ii) the distinct structural features and functional mechanisms among these protein classes can influence the ability of the model to capture relevant information and make accurate predictions. The features selected for the generalized model may not be equally important across all functional classes, leading to suboptimal performance in certain cases. Supplementary Figure S5 shows the varying importance of features across functional classes suggesting that different classes rely on specific sets of features

for accurate predictions. This can be overcome by developing separate models for each functional class upon the availability of a sufficient number of data in each class.

In the blind set, mutations in enzymes, receptors, transporters, and miscellaneous proteins showed MAE values of 0.82, 0.80, 0.70, and 0.78, respectively. Overall, the model demonstrates robust performance across all functional classes, with an MAE of <1 kcal/mol in each class, indicating the generalizability of the model.

Comparative analysis of $\Delta\Delta G$ s between membrane and globular proteins

A detailed comparison between experimental and predicted $\Delta\Delta G$ values across different amino acid types is plotted in Fig. 3. We categorized the amino acid residues into charged (R,H,K,D,E), polar (S,T,N,Q), hydrophobic (A,V,I,L,M,F,Y,W), and special groups (C,G,P). From Fig. 3a and b, it is interesting to note that most mutations, particularly those involving charged and hydrophobic groups mutating to alanine, have a positive affinity change except for one mutation (Gly to Ala). For instance, charged residues at the interface contribute to electrostatic interactions, while bulky hydrophobic residues play a crucial role in stabilizing protein-protein complexes through hydrophobic interactions. Replacing these residues with Ala disrupts these interactions, leading to the destabilization of the complex and a decrease in binding affinity [28]. This observation is similar to that found in globular protein-protein complexes [15] as shown in Fig. 3c. It may be due to the fact that our dataset also contains complexes, where binding occurs in the extracellular and/or cytoplasmic regions.

Furthermore, we performed a qualitative analysis focusing on the proportion of mutations decreasing the binding affinity (denoted by positive $\Delta\Delta G$). Similar to the above observation, most mutations to Ala have $>70\%$ positive $\Delta\Delta G$ (Supplementary Figures S6a and b). A similar pattern is observed in globular protein complexes also (Supplementary Figure S6c). Thus, we observe a consistent trend based on average $\Delta\Delta G$ and % of mutations decreasing (or increasing) the binding affinity, confirming the reliability of our observations.

On examining the $\Delta\Delta G$ values, we observe that the majority of mutations to arginine have a negative free energy change

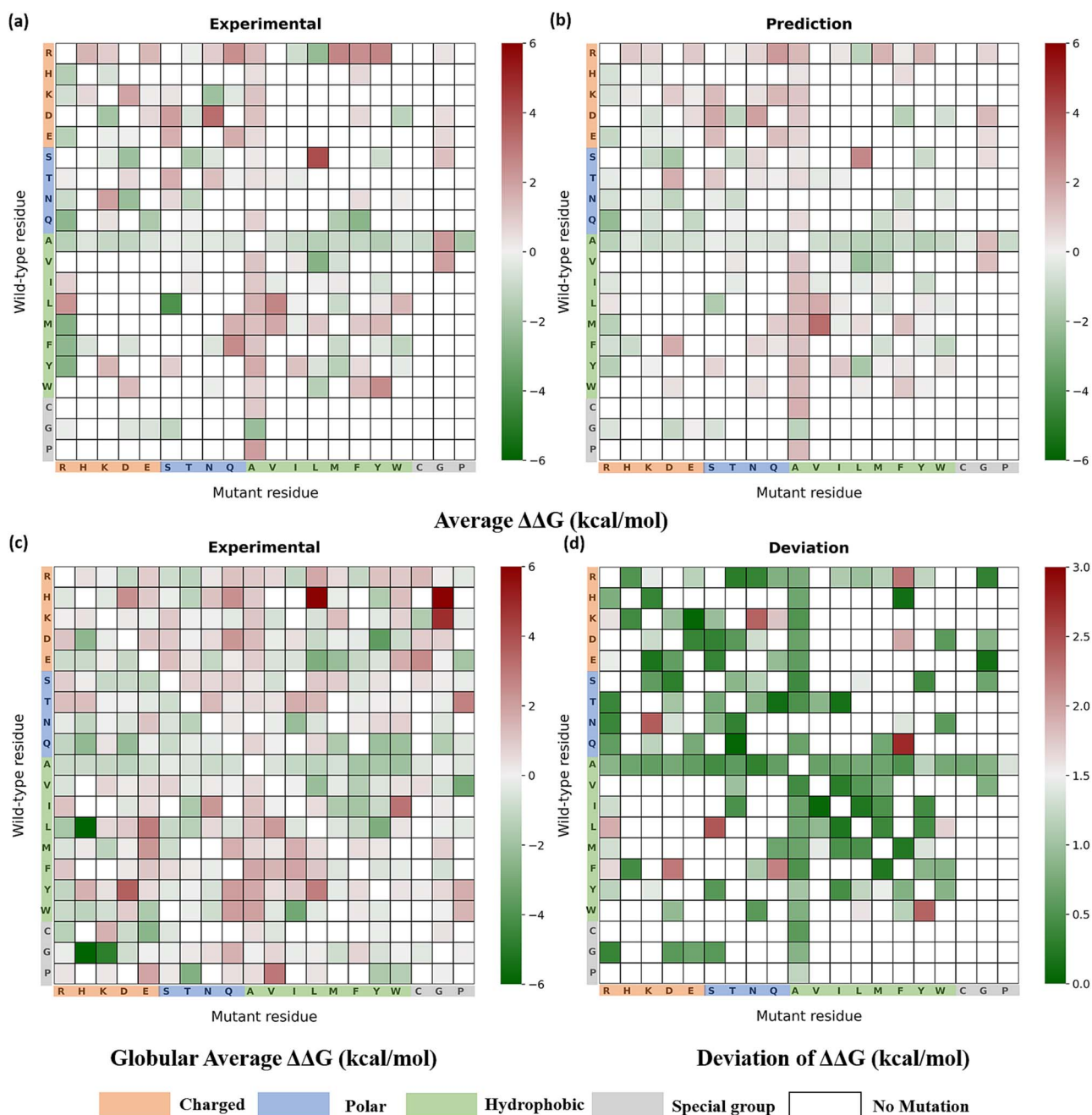


Figure 3. A comparative analysis of mutation-induced binding affinity changes across various amino acid types. (a) and (b) are experimental and predicted average binding affinity changes upon mutation (kcal/mol) respectively, (c) is average $\Delta\Delta G$ for the globular protein dataset, while (d) is the deviation between experimental and predicted $\Delta\Delta G$ (jack-knife test) upon each type of mutation (kcal/mol) in MP complexes. The figure uses distinct color codes to represent different amino acid groups: charged (R,H,K,D,E), polar (S,T,N,Q), hydrophobic (A,V,I,L,M,F,Y,W), special groups (C,G,P), and positions with no mutations.

indicating an increase in binding affinity, possibly due to favorable electrostatic interactions with the oppositely charged groups on the binding partner, strengthening the binding. This agrees with a previous study [29] that positive charges contribute to stabilizing protein–protein interfaces through favorable electrostatic interactions. An illustrative instance is the mutation Q33R within the IFNa2-ifnar2 complex (PDB:3S9D), where the substitution to Arg introduces an electrostatic interaction between Arg 33 and Asp 51, which was absent in the wild-type complex (Supplementary Figure S7).

Overall, comparing the patterns in Fig. 3a and b shows that our predictions are in close agreement with the experimental data in

terms of average $\Delta\Delta G$ values. Figure 3d shows that 90% of the mutations fall within a deviation of 1.5 kcal/mol, indicating a high level of agreement between the experimental and predicted $\Delta\Delta G$. This consistency underscores the reliability and accuracy of our prediction model in capturing the change in binding affinity upon mutation.

Analysis of features influencing $\Delta\Delta G$ prediction

The final set of features selected for our model includes accessible surface area, energetic parameters obtained using FoldX such as total energy, electrostatics, and solvation; interface contacts, PSSM score, buriedness, long-range nonbonded energy, and degree

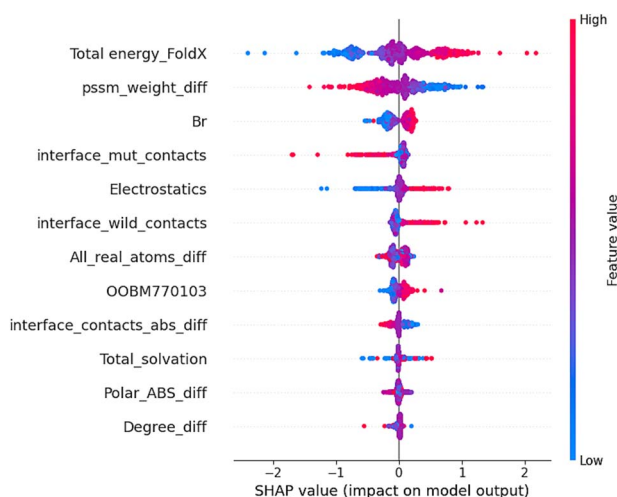


Figure 4. Beeswarm plot showing the SHAP analysis of the $\Delta\Delta G$ prediction model, where features are ranked in descending order of importance according to their SHAP scores.

(network property). To understand the impact of individual features on the prediction of $\Delta\Delta G$, we performed feature ablation and SHAP analysis [30].

Feature ablation study

In order to assess the importance of each feature, we conducted a feature ablation study by systematically removing each feature from the model and evaluating its impact on the prediction performance of $\Delta\Delta G$. This process helped identify the contribution of each feature to the overall model performance. [Supplementary Figure S8](#) displays the jack-knife test performance of the ablated features in terms of correlation and MAE for $\Delta\Delta G$ prediction. The results demonstrate that excluding one or both “pssm_weight_diff” and “Total energy_FoldX” features showed a significant performance drop ($r=0.63$ and $MAE=0.87$ kcal/mol), highlighting the importance of these features for our prediction. In contrast, we observed that the elimination of other features reduced the performance minimally ($MAE < 0.05$ kcal/mol).

SHapley Additive exPlanations analysis

The importance of each feature in the model was assessed and ranked using SHAP analysis [30] to evaluate their contributions to the model prediction. SHAP assigns an importance score to each feature that quantifies its positive or negative impact on the final prediction, providing a clear understanding of how each feature affects the outcome. A higher SHAP score denotes greater feature importance, whereas a lower score indicates reduced importance. The beeswarm plot derived from the SHAP analysis is provided in [Fig. 4](#).

The important features influencing the binding affinity change are discussed in detail below.

Energetic parameters

The ablation and SHAP analysis revealed that the change in overall stability energy (Total energy_FoldX) obtained from FoldX is the most important feature, exhibiting nonlinear relationships with the model output as evidenced by their wide range of both positive and negative SHAP values. This prominence is consistent with findings from a previous study where the thermodynamic stability of complexes was an important feature for the prediction

of affinity changes upon mutations [10]. Analyzing [Fig. 5a](#), we observed a direct relationship between stability change and $\Delta\Delta G$. This observation is further substantiated by an example of Y13A mutation in the interleukin-4/receptor alpha chain complex (PDB: 1IAR). The positive $\Delta\Delta G$ of 5.2 kcal/mol indicates a weaker binding affinity compared to the wild type, which showed a good agreement with the observed decrease in stability change of 6.3 kcal/mol. These observations demonstrate how total stability energy difference correlates with the binding affinity change.

Another selected feature from FoldX is the solvation energy, which includes both polar and nonpolar solvation energy. This agrees with the previous study [31] which reports a crucial role of solvation energy in determining the binding affinity changes. Interestingly, our data revealed that mutations leading to stronger binding affinity (negative $\Delta\Delta G$) were accompanied by a positive solvation energy difference ($\Delta\Delta G_{solv}$). While the mutation might disrupt favorable interactions with solvent molecules (positive $\Delta\Delta G_{solv}$), it could also lead to the formation of new favorable interactions between the proteins (e.g. hydrogen bonds, van der Waals forces) that outweigh the solvation penalty, leading to a net increase in binding affinity (negative $\Delta\Delta G$).

Change in electrostatic interaction energy feature from FoldX as shown in [Fig. 5b](#), depicts that mutations leading to more favorable electrostatic interactions (more negative $\Delta\Delta E_{elec}$) might tend to shift toward the left (more negative $\Delta\Delta G$) on the graph, potentially indicating stronger binding affinity. This suggests that electrostatic interactions can influence the binding affinity change upon mutation.

Solvent accessibility

Change in relative solvent accessibility (ΔASA_{rel}) is another important feature. We observed a negative correlation between $\Delta\Delta G$ and ΔASA_{rel} , which implies that mutations leading to decreased solvent accessibility (negative ΔASA_{rel}) tend to be associated with stronger binding affinity (negative $\Delta\Delta G$). This observation can be explained by the reduced competition from water molecules for binding interactions when solvent accessibility decreases. Consequently, stronger interactions can form between the mutated protein and its binding partner protein, leading to increased binding affinity. Previous studies have also highlighted this feature as a crucial factor in predicting $\Delta\Delta G$ [9, 32]. A similar trend was observed for the change in polar ASA, which was also a feature selected, suggesting a potential role of polar group accessibility in influencing binding affinity.

Interface contacts

The number of contacts in the interface is another important feature influencing the binding affinity. The SHAP plot shows that an increase in the number of mutant interface contacts is associated with increased affinity (negative SHAP value), while an increase in the number of wild-type interface contacts correlates with decreased affinity. [Figure 5c](#), depicting the change in the number of contacts between wild and mutant residue, shows that mutations increasing the number of contacts (positive $\Delta Contact$) tend to be associated with a stronger binding affinity (negative $\Delta\Delta G$). This aligns with the concept that forming more contacts often leads to a larger interaction surface area between the protein and its binding partner. This, in turn, can facilitate the formation of favorable interactions such as hydrogen bonds and electrostatic interactions, contributing to a more stable complex and potentially lowering the binding free energy (negative $\Delta\Delta G$).

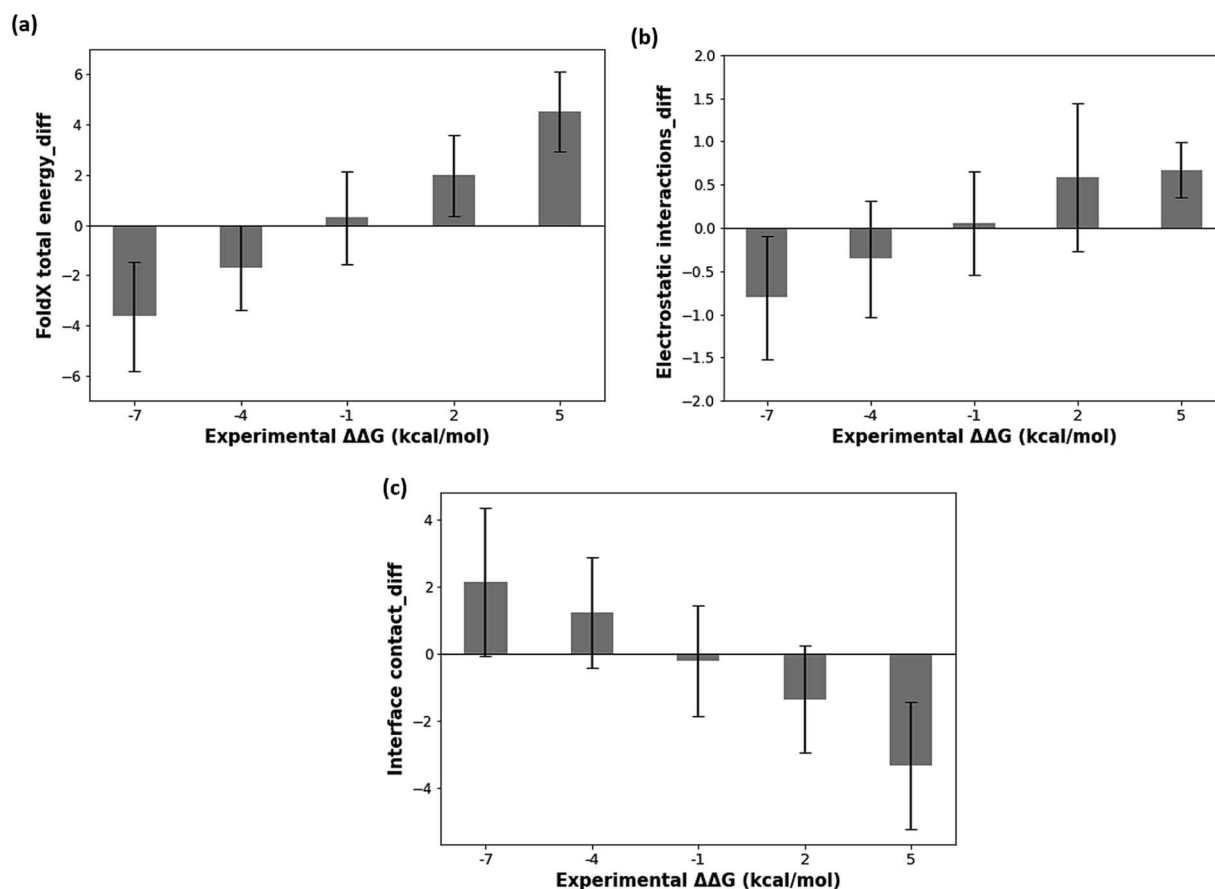


Figure 5. Distribution of various features across different $\Delta\Delta G$ ranges (steps of 3 kcal/mol) (a) change in FoldX total energy (b) change in electrostatic interaction energy, and (c) change in number of contacts in the interface.

Sequence-based features

Among the sequence-based features, the difference in weighted PSSM score between mutant and wildtype residues (`pssm_weight_diff`) was found to be the most important feature, as reported in a previous study [33] and confirmed by the ablation study. It signifies the extent of change introduced by the mutation in terms of evolutionary conservation at the position of interest. Analysis of the SHAP plot indicates that higher “`pssm_weight_diff`” tends to yield negative SHAP values, implying that mutating a less conserved residue to more conserved residues leads to increased binding affinity. Conversely, lower “`pssm_weight_diff`” values are associated with positive SHAP values, indicating decreased binding affinity. This highlights the significance of conservation in predicting the impact of mutations on protein binding affinity.

Other sequence-based features such as buriedness and long-range nonbonded energy were also key for predicting the effect of mutations on binding affinity.

Discrimination of high- and low-affinity mutation

We attempted to utilize the predicted $\Delta\Delta G$ values for discriminating high- and low-affinity mutations in the MP–protein complexes. We classified the mutations as increasing ($\Delta\Delta G < 0$) and decreasing ($\Delta\Delta G \geq 0$) affinity [8]. The classification performance revealed that the developed model achieved a sensitivity of 81% and a specificity of 80%, with an overall accuracy of 80%.

Comparison of prediction performance with existing methods

We initially employed the simple average assignment method [34] to predict binding affinity changes upon mutation. This method involved averaging affinities within mutation groups (e.g. Ala to Val) and assigning the same average affinity to all mutations within each group. It yielded a slightly lower MAE (0.7 kcal/mol) than our ML model (0.73 kcal/mol). However, upon further investigation, we found that the average assignment method resulted in an MAE of zero for mutations with only one data point ($n=71$), limiting its ability to capture individual mutation effects. After removing them, the MAE increased to 0.77 kcal/mol in training and 1.41 kcal/mol in the jack-knife test. Additionally, for proteins with a greater number of mutations (>5), we observed that the MAE is 1.13 kcal/mol in the jack-knife test, while our method showed an MAE of 0.70 kcal/mol. Thus, our model addresses the limitations and outperforms the average assignment method, resulting in a more accurate prediction.

We assessed our method by comparing its performance with existing ML-based methods including `Mscm-PPI2` [9], `SAAMBE-3D` [12], and `SAAMBE-SEQ` [13], as well as deep learning-based methods such as `GeoPPI` [14], and `DDMut-PPI` [16], with the results shown in Table 1 and Supplementary Figure S9. The analysis revealed that our method achieved an MAE of 0.77 kcal/mol in predicting $\Delta\Delta G$, outperforming other methods, which showed an MAE of ≥ 1 kcal/mol. Additionally, while these methods exhibited correlations in the range of 0.4–0.7, our method demonstrated a superior correlation of 0.85. The improved performance of the

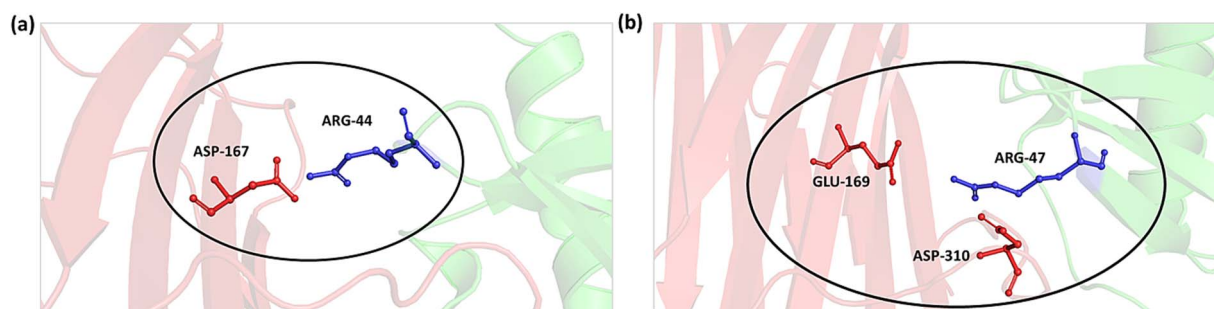


Figure 6. Structure of SECRET/CX3CL1 complex (3ONA), where (a) Arg 44 – Asp 167, and (b) Arg 47 – Asp 310 and Arg 47 – Glu 169, form electrostatic interactions in the interface.

Table 1. Comparative evaluation of performance with existing methods on the blind dataset.

Method	r	MAE (kcal/mol)
mCSM-PPI2	0.67	1.12
SAAMBE-3D	0.38	1.68
SAAMBE-SEQ	0.43	1.51
DDMut-PPI	0.74	0.96
GeoPPI	0.53	1.28
MPA-MutPred (our work)	0.85	0.77

method can be due to the fact that it is specifically designed for mutations in MP–protein complexes, while others are for protein–protein complexes in general. Our model incorporates a unique combination of both structure- and sequence-based features that specifically capture the biophysical properties of MP interfaces.

We also attempted to compare the performance with MPA-Pred by predicting the wild-type and mutant ΔG values for the MP complexes and then calculating $\Delta\Delta G$ using Equation (1). However, the average MAE obtained with MPA-Pred is >2 kcal/mol when compared to the present method, which is 0.77 kcal/mol. This result indicates that our method, tailored specifically for assessing binding affinity changes due to mutations in MP complexes, performs better than MPA-Pred.

Case study: SECRET/CX3CL1 complex

The SECRET domain in complex with the chemokine CX3CL1 plays a critical role in the immune evasion strategy of the viruses causing smallpox [35]. Figure 6 shows the structure of SECRET/CX3CL1 complex (3ONA). Mutating the charged residue Arg 44 to Ala (R44A) results in an experimental $\Delta\Delta G$ of 1.88 kcal/mol, which our method predicted as 1.56 kcal/mol, demonstrating a close alignment with the experimental value. Positive $\Delta\Delta G$ indicates that the mutation has caused a decrease in the binding affinity. A careful analysis of the structure revealed that there is electrostatic interaction between Arg 44 and Asp 167 in the wild type, which is lost in the mutant structure, which is Ala 44. Also, the mutation caused the relative ASA to be more than the wild type, reducing the binding affinity. For the R47A mutation, with an experimental $\Delta\Delta G$ of 2.36 kcal/mol, our method estimated the $\Delta\Delta G$ to be 2.14 kcal/mol, showing a deviation of 0.21 kcal/mol. This mutation also led to a significant reduction in binding affinity, highlighting the critical role of salt-bridge interactions in the formation of the complex. For the reverse mutation A47R, our method predicted the $\Delta\Delta G$ as -1.72 kcal/mol. The combination of the selected parameters likely

enabled accurate predictions of the $\Delta\Delta G$, with deviations within 1 kcal/mol.

Prediction on the web

MPA-MutPred is available as a free and user-friendly web server, accessible at <https://web.iitm.ac.in/bioinfo2/MPA-MutPred/>. To submit a prediction job, users need to provide the MP complex structure by either entering a valid PDB ID or uploading a PDB file. Users also have to provide the interacting chains and mutation information. The output page predicts and displays the $\Delta\Delta G$ value. The tutorials page on the web server provides prediction examples and instructions for the supported input file formats.

Conclusions

This study introduces a novel method for predicting the mutation-induced changes in the binding affinity of MP–protein complexes. Breaking from conventional approaches, our method harnesses the strengths of both linear and nonlinear models, potentially leading to a more robust model for predicting the $\Delta\Delta G$. While MLR explicitly identifies informative features, a nonlinear model helps to capture complex relationships between the features to make more accurate predictions. This novel approach holds significant promise in the realm of interpretable artificial intelligence by achieving a balance between prediction accuracy and interpretability.

Our extensive analysis of the features revealed that change in the stability of the complex, conservation of the site, electrostatic interaction, relative solvent accessibility, and interface contacts are crucial for accurately predicting the binding affinity in MP complexes. The method achieved a correlation of 0.75 and an MAE of 0.73 kcal/mol in the jack-knife test. In the test set, it achieved a higher correlation of 0.85 and an MAE of 0.77 kcal/mol for predicting changes in binding free energy caused by mutations. While the method has demonstrated a good performance, it has few limitations, which is mainly the scarcity of experimental affinity data across diverse mutations, with some mutation types having none or few data points. The under-representation of certain mutation types in our dataset may impact the generalizability of the model. This issue could be addressed with the availability of more representative mutation data in the future.

Further, we also developed a web server for $\Delta\Delta G$ prediction in MP complexes, designed to assist with large-scale analyses. We believe that our work will serve as a useful resource for understanding the relationship between changes in binding affinity and disease-causing mutations, elucidating the mechanisms underlying specific diseases, and thereby aiding in targeted drug design.

Key Points

- Developed a novel machine-learning approach for predicting mutation-induced changes in membrane protein binding affinities.
- The method harnesses the strengths of both linear and nonlinear models, leading to a more robust model for prediction.
- Changes in the stability of the complex, conservation score, electrostatic interaction, relative solvent accessibility, and interface contacts are important for prediction.
- Our method achieved a correlation of 0.75 and an MAE of 0.73 kcal/mol in the jack-knife test.
- Developed a web server for predicting the $\Delta\Delta G$ in MP complexes for large-scale analysis.

Supplementary data

Supplementary data are available at *Briefings in Bioinformatics* online.

Acknowledgements

We are thankful to IIT Madras for offering computational support. We also appreciate the insightful suggestions and discussions from members of the PBI Lab.

Author contributions

Fathima Ridha (Data Curation, Model Development, Validation, Formal analysis, Software, Writing—Original Draft, Writing—Review & Editing, Visualization) and M. Michael Gromiha (Conceptualization, Methodology, Validation, Investigation, Resources, Writing—Review & Editing, Supervision).

Funding

Ministry of Education, India for PMRF scholarship to F.R. The work is partially supported by the DBT, India to M.M.G. (BT/PR40237/BTIS/137/79/2023).

Data availability

The website is freely accessible to all users, and the dataset used can be found on the website. We have also provided the GitHub code at <https://github.com/Fathima-Ridha/MPA-MutPred>.

References

1. Almén MS, Nordström KJ, Fredriksson R. *et al.* Mapping the human membrane proteome: A majority of the human membrane proteins can be classified according to function and evolutionary origin. *BMC Biol* 2009;**7**:50.
2. Almeida JG, Preto AJ, Koukos PI. *et al.* Membrane proteins structures: a review on computational modeling tools. *Biochim Biophys Acta Biomembr* 2017;**1859**:2021–39. <https://doi.org/10.1016/j.bbmem.2017.07.008>.
3. Ridha F, Gromiha MM. MPA-Pred: a machine learning approach for predicting the binding affinity of membrane protein-protein complexes. *Proteins* 2024;**92**:499–508. <https://doi.org/10.1002/prot.26633>.
4. Berezovsky IN. The diversity of physical forces and mechanisms in intermolecular interactions. *Phys Biol* 2011;**8**:035002. <https://doi.org/10.1088/1478-3975/8/3/035002>.
5. Kulandaisamy A, Ridha F, Frishman D. *et al.* Computational approaches for investigating disease-causing mutations in membrane proteins: database development, analysis and prediction. *Curr Top Med Chem* 2022;**22**:1766–75. <https://doi.org/10.2174/1568026622666220726124705>.
6. Cordeiro JM, Brugada R, Wu YS. *et al.* Modulation of I(Kr) inactivation by mutation N588K in KCNH2: a link to arrhythmogenesis in short QT syndrome. *Cardiovasc Res* 2005;**67**:498–509.
7. Huang SF, Liu HP, Li LH. *et al.* High frequency of epidermal growth factor receptor mutations with complex patterns in non-small cell lung cancers related to gefitinib responsiveness in Taiwan. *Clin Cancer Res J Am Assoc Cancer Res* 2004;**10**:8195–203.
8. Ridha F, Kulandaisamy A, Michael Gromiha M. MPAD: a database for binding affinity of membrane protein-protein complexes and their mutants. *J Mol Biol* 2023;**435**:167870. <https://doi.org/10.1016/j.jmb.2022.167870>.
9. Rodrigues CHM, Myung Y, Pires DEV. *et al.* mCSM-PPI2: predicting the effects of mutations on protein-protein interactions. *Nucleic Acids Res* 2019;**47**:W338–44. <https://doi.org/10.1093/nar/gkz383>.
10. Zhang N, Chen Y, Lu H. *et al.* MutaBind2: predicting the impacts of single and multiple mutations on protein-protein interactions. *iScience* 2020;**23**:100939. <https://doi.org/10.1016/j.isci.2020.100939>.
11. Wang M, Cang Z, Wei GW. A topology-based network tree for the prediction of protein-protein binding affinity changes following mutation. *Nat Mach Intell* 2020;**2**:116–23. <https://doi.org/10.1038/s42256-020-0149-6>.
12. Pahari S, Li G, Murthy AK. *et al.* SAAMBE-3D: predicting effect of mutations on protein-protein interactions. *Int J Mol Sci* 2020;**21**:2563.
13. Li G, Pahari S, Murthy AK. *et al.* SAAMBE-SEQ: a sequence-based method for predicting mutation effect on protein-protein binding affinity. *Bioinformatics (Oxford, England)* 2021;**37**:992–9. <https://doi.org/10.1093/bioinformatics/btaa761>.
14. Liu X, Luo Y, Li P. *et al.* Deep geometric representations for modeling effects of mutations on protein-protein binding affinity. *PLoS Comput Biol* 2021;**17**:e1009284. <https://doi.org/10.1371/journal.pcbi.1009284>.
15. Nikam R, Jemimah S, Gromiha MM. DeepPPAPredMut: deep ensemble method for predicting the binding affinity change in protein-protein complexes upon mutation. *Bioinformatics (Oxford, England)* 2024;**40**:btac309.
16. Zhou Y, Myung Y, Rodrigues CHM. *et al.* DDMut-PPI: predicting effects of mutations on protein-protein interactions using graph-based deep learning. *Nucleic Acids Res* 2024;**52**:W207–14. <https://doi.org/10.1093/nar/gkac412>.
17. Schmidt PJ, Toran PT, Giannetti AM. *et al.* The transferin receptor modulates Hfe-dependent regulation of hepcidin expression. *Cell Metab* 2008;**7**:205–14. <https://doi.org/10.1016/j.cmet.2007.11.016>.
18. Tsishyn M, Pucci F, Rooman M. Quantification of biases in predictions of protein-protein binding affinity changes upon mutations. *Brief Bioinform* 2023;**25**:bbad491.
19. Schymkowitz J, Borg J, Stricher F. *et al.* The FoldX web server: an online force field. *Nucleic Acids Res* 2005;**33**:W382–8.

20. Hubbard SJ, Thornton JM. NACCESS. Computer Program, Department of Biochemistry and Molecular Biology, University College London, 1993.
21. McDonald IK, Thornton JM. Satisfying hydrogen bonding potential in proteins. *J Mol Biol* 1994;**238**:777–93.
22. Hagberg A, Swart PJ, Schult DA. *Exploring Network Structure, Dynamics, and Function Using Networkx. Technical Report*. Los Alamos, NM, USA: Los Alamos National Lab (LANL), 2008.
23. Kawashima S, Pokarowski P, Pokarowska M. et al. AAindex: amino acid index database, progress report 2008. *Nucleic Acids Res* 2008;**36**:D202–5.
24. Valdar WS. Scoring residue conservation. *Proteins* 2002;**48**: 227–41.
25. Pedregosa F, Varoquaux G, Gramfort A. et al. Scikit-learn: machine learning in python. *J Mach Learn Res* 2011;**12**: 2825–30.
26. Piehler J, Roisman LC, Schreiber G. New structural and functional aspects of the type I interferon-receptor interaction revealed by comprehensive mutational analysis of the binding interface. *J Biol Chem* 2000;**275**:40425–33.
27. Zhang JL, Simeonowa I, Wang Y. et al. The high-affinity interaction of human IL-4 and the receptor alpha chain is constituted by two independent binding clusters. *J Mol Biol* 2002;**315**: 399–407.
28. Akasako A, Haruki M, Oobatake M. et al. Conformational stabilities of Escherichia coli RNase HI variants with a series of amino acid substitutions at a cavity within the hydrophobic core. *J Biol Chem* 1997;**272**:18686–93.
29. Ma BG, Goncarenco A, Berezovsky IN. Thermophilic adaptation of protein complexes inferred from proteomic homology modeling. *Structure (London, England)* 2010, 1993;**18**: 819–28.
30. Lundberg S, Lee S. A unified approach to interpreting model predictions. *ArXiv* 2017; arXiv:1705.07874.
31. Li M, Petukh M, Alexov E. et al. Predicting the impact of missense mutations on protein-protein binding affinity. *J Chem Theory Comput* 2014;**10**:1770–80.
32. Brender JR, Zhang Y. Predicting the effect of mutations on protein-protein binding interactions through structure-based interface profiles. *PLoS Comput Biol* 2015;**11**:e1004494. <https://doi.org/10.1371/journal.pcbi.1004494>.
33. Geng C, Vangone A, Folkers GE. et al. iSEE: interface structure, evolution, and energy-based machine learning predictor of binding affinity changes upon mutations. *Proteins* 2019;**87**:110–9. <https://doi.org/10.1002/prot.25630>.
34. Saraboji K, Gromiha MM, Ponnuswamy MN. Average assignment method for predicting the stability of protein mutants. *Biopolymers* 2006;**82**:80–92.
35. Xue X, Lu Q, Wei H. et al. Structural basis of chemokine sequestration by CrmD, a poxvirus-encoded tumor necrosis factor receptor. *PLoS Pathog* 2011;**7**:e1002162. <https://doi.org/10.1371/journal.ppat.1002162>.